Development/Plasticity/Repair

Hippocampal Synaptic Metaplasticity Requires Inhibitory Autophosphorylation of Ca^{2+}/Calmodulin-Dependent Kinase II

Lian Zhang,[1,2] Timo Kirschstein,[1] Britta Sommersberg,[1] Malte Merkens,[1] Denise Manahan-Vaughan,[3,4] Ype Elgersma,[5] and Heinz Beck[1]

[1]Department of Epileptology, University of Bonn, D-53105 Bonn, Germany, [2]Department of Pediatrics, Tongji Hospital, Huazhong University of Science and Technology, Wuhan 430030, China, [3]Learning and Memory Research, International Graduate School of Neuroscience, Ruhr University Bochum, 44780 Bochum, Germany, [4]Institute for Physiology, Humboldt University Medical Faculty (Charité), 10117 Berlin, Germany, and [5]Department of Neuroscience, Erasmus Medical Center, University Rotterdam, 3000 DR Rotterdam, The Netherlands

Virtually all CNS synapses display the potential for activity-dependent long-term potentiation (LTP) and/or long-term depression (LTD). Intriguingly, the potential to exhibit LTP or LTD at many central synapses itself is powerfully modulated by previous synaptic activity. This higher-order form of plasticity has been termed metaplasticity. Here, we show that inhibitory autophosphorylation of Ca^{2+}/calmodulin-dependent kinase II (CaMKII) is required for hippocampal metaplasticity at the lateral perforant path–dentate granule cell synapse. Brief 10 Hz priming, which does not affect basal synaptic transmission, caused a dramatic, pathway-specific and long-lasting (up to 18 h) reduction in subsequently evoked LTP at lateral perforant path synapses. In contrast, LTD was unaffected by priming. The induction of lateral perforant path metaplasticity required the activation of NMDA receptors during priming. In addition, metaplasticity was absent in knock-in mice expressing αCaMKII that cannot undergo inhibitory phosphorylation, indicating that inhibitory autophosphorylation of αCaMKII at threonines 305/306 is required for metaplasticity. Metaplasticity was not observed in the medial perforant pathway, consistent with the observation that CaMKII activity was not required for the induction of LTP at this synapse. Thus, modulation of αCaMKII activity via autophosphorylation at Thr305/Thr306 is a key mechanism for metaplasticity that may be of importance in the integration of temporally separated episodes of activity.

Key words: **metaplasticity; LTP; LTD; Ca^{2+}/calmodulin-dependent kinase II; hippocampus; autophosphorylation**

Introduction

The ability to modify synaptic strength in an activity-dependent manner, either as long-term depression (LTD) or long-term potentiation (LTP), is a fundamental feature of most CNS synapses. A less well studied but particularly intriguing finding is that the capacity of many synapses for plastic changes itself is subject to considerable activity-dependent variation, or plasticity. This higher-order plasticity has been termed metaplasticity (Deisseroth et al., 1995; Abraham and Bear, 1996). Importantly, induction of metaplasticity does not necessarily lead to changes in synaptic strength per se but rather modifies the ability of synapses to exhibit synaptic plasticity in response to subsequent episodes of synaptic activity. For instance, a number of studies have demonstrated an inhibition of LTP after priming stimulation with frequencies ranging from 5 to 30 Hz (Huang et al., 1992; O'Dell and Kandel, 1994; Christie et al., 1995; Wang and Wagner, 1999). Stimulation within the same frequency range was also shown to enhance subsequent LTD (Christie and Abraham, 1992). Conversely, a facilitation of LTP after metabotropic glutamate receptor (mGluR) activation has been described (Bortolotto et al., 1994; Manahan-Vaughan and Reymann, 1996; Cohen et al., 1998). It was proposed on theoretical grounds that the expression of metaplasticity may consist of an activity-dependent shift of the transition threshold θ_m between LTD and LTP toward higher or lower stimulation intensities (Bienenstock et al., 1982), an idea for which experimental support was subsequently provided (Bear et al., 1987). Metaplasticity has been suggested to play an important role in normal neuronal function to keep synapses within a dynamic functional range, thus preventing them from entering states of saturated LTP or LTD (Abraham and Tate, 1997). It is particularly interesting to note that facilitation of LTD can also be induced by an alteration of behavioral state (Xu et al., 1998), indicating that metaplastic processes are invoked and may be important during normal behavior.

Despite the potential importance of metaplasticity, not much is known about the underlying cellular and molecular mecha-

Received Feb. 14, 2005; revised July 4, 2005; accepted July 4, 2005.

This work was supported by Deutsche Forschungsgemeinschaft Sonderforschungsbereich Tr3/C4 (D.M.-V., H.B.) and by a grant of the National Epilepsy Fund, "The Power of the Small" (Y.E.). We are grateful to Jens Klausnitzer for technical support.

Correspondence should be addressed to Heinz Beck, Department of Epileptology, University of Bonn, Sigmund-Freud-Strasse 25, D-53105 Bonn, Germany. E-mail: heinz.beck@ukb.uni-bonn.de.

DOI:10.1523/JNEUROSCI.2086-05.2005

 0270-6474/05/257697-11$15.00/0

nisms. Several lines of evidence indicate that α Ca^{2+}/calmodulin-dependent kinase II (αCaMKII) may be a promising candidate to mediate metaplasticity. After activation of αCaMKII by Ca^{2+} influx, activation is maintained by autophosphorylation at threonine 286, even after intracellular Ca^{2+} has returned to baseline levels (for review, see Lisman et al., 2002). This autophosphorylation has been shown to be required for LTP induction and spatial learning (Giese et al., 1998). Autophosphorylation at Thr305/306, conversely, interferes with the binding of calcium/calmodulin, thereby blocking the activation of CaMKII activity *in vitro* (Colbran and Soderling, 1990; Patton et al., 1990; Mukherji and Soderling, 1994). In addition, autophosphorylation at Thr305/306 was shown to regulate αCaMKII association with the postsynaptic density (PSD), which is essential for controlling hippocampal LTP and learning (Elgersma et al., 2002). Thus, CaMKII is bidirectionally regulated by activity and, in turn, profoundly affects synaptic plasticity. Thus, it appears likely that CaMKII could be a pivotal component in the bidirectional modulation of synaptic efficacy. In the present study, we characterize metaplasticity at the perforant path–dentate granule cell synapse and demonstrate a role for αCaMKII inhibitory autophosphorylation in this phenomenon.

Materials and Methods

αCaMKII mutant mice. The αCaMKII TT305/306VA point mutant has been described previously (Elgersma et al., 2002). Mutant mice were backcrossed 11 times with C57BL/6J. These mice were then crossed once with 129/Sv (Charles River, Maastricht, The Netherlands). Heterozygous offspring of these mice were crossed with each other to obtain homozygous mutants and wild-type littermates in the F2 hybrid C57BL/6/129Sv background. Adult mice (10–14 weeks) were used for slice electrophysiology as described below.

Slice preparation. Adult male Wistar rats (30–40 d old; 80–150 g) or mice (see above) were anesthetized with diethylether and decapitated. The brain was removed and immediately immersed in ice-cold carbogenated ($95\%O_2/5\%CO_2$) dissection saline that contained the following (in mM): 125.0 NaCl, 3.0 KCl, 0.2 $CaCl_2$, 5.0 $MgSO_4$, 1.25 NaH_2PO_4, 26.0 $NaHCO_3$, and 13.0 D-glucose. Transverse slices (400 μm) were prepared with a vibratome (VT1000S; Leica, Wetzlar, Germany) and transferred to an interface chamber in which they were continuously superfused (1.8 ml/min) with artificial CSF (ACSF) containing the following (in mM): 125.0 NaCl, 3.0 KCl, 2.5 $CaCl_2$, 1.3 $MgCl_2$, 1.25 NaH_2PO_4, 26.0 $NaHCO_3$, and 13.0 D-glucose, pH 7.35 (osmolality 300–308 mOsm/kg in all solutions). The temperature of the recording chamber was maintained at 35°C. The slices were allowed to recover for at least 1 h before starting recordings.

Electrophysiology. Extracellular borosilicate glass recording microelectrodes (~2 MΩ) were filled with extracellular ACSF. The recording electrodes were placed within the outer and middle molecular layer for recording of lateral and medial perforant path field EPSPs (fEPSPs), respectively. Stimulation of the lateral and medial aspects of the perforant path was performed by placing bipolar stimulating electrodes within the outer and the middle molecular layer, respectively. The electrode positions were adjusted so that stimulation of the lateral perforant path caused a current sink in the outer molecular layer and a source in the middle molecular layer and vice versa for stimulation of the medial perforant path (see Fig. 2*A*). As an additional criterion, lateral perforant path responses showed paired-pulse facilitation, whereas medial perforant path responses displayed paired-pulse inhibition (40 ms interpulse interval). This configuration was usually readily obtained. In some experiments, the identity of lateral perforant path recordings was confirmed pharmacologically by applying the selective group III mGluR agonist (L)-2-amino-2-methyl-4-phosphonobutyrate (L-AP-4) (10 μM). Stimulation was performed with square impulses of 50–200 μA lasting 0.1 ms via a stimulus isolator (World Precision Instruments, Sarasota, FL). Data were digitized at 10 kHz and analyzed with pClamp 8 software (Molecular Devices, Foster City, CA). Stimulus response curves were performed at the beginning of each experiment. The stimulus strength was then adjusted to yield fEPSPs that were 40–60% of the maximum response, and stimuli were applied at a frequency of 0.025 Hz for the remainder of the experiment. In some experiments, antidromic stimulation was performed by placing a stimulation electrode within the dentate hilar region.

Priming and conditioning stimuli. Priming stimulation *in vitro* was performed at 10 Hz (10 episodes of 20 pulses, spaced 1 s apart) in all homosynaptic, heterosynaptic, and antidromic priming experiments. Subsequent conditioning stimulation was performed with the same number of stimuli and spacing of episodes at frequencies ranging from 1 to 400 Hz. Both priming and conditioning stimulation were performed with a stimulation strength increased twofold compared with the baseline stimulation strength. In those cases in which priming stimulation caused a significant change of fEPSP amplitude, the stimulation strength was adjusted to prepriming baseline levels during the last 20 min before applying a conditioning tetanus.

Data analysis. To analyze synaptic efficacy, the maximal slope was determined in the rising phase of fEPSPs. Values from three successive fEPSPs were averaged to yield one data point. To determine the amount of LTP or LTD in the different experimental groups, we first determined as the average value of the fEPSP slope of the three last fEPSPs during the follow-up period, i.e., 60 min after conditioning stimulation. All values were normalized to the average fEPSP slope of the first 10 min of the baseline recording period, such that values >1 indicate potentiation and values <1 indicate depression. This value was then related to the average fEPSP slope during baseline recording. All data are expressed as mean ± SEM. Statistical comparisons were performed using Mann–Whitney *U* test with $p < 0.05$ as the threshold for statistical significance.

Drugs and reagents. All salts were obtained from Sigma (Deisenhofen, Germany). D(−)-2-amino-5-phosphonovaleric acid (APV) and L-AP-4 were purchased from Tocris Cookson (Bristol, UK), and *R*-(−)-2-amino-3-hydroxypropionic acid was obtained from Sigma. The latter drugs were dissolved in double-distilled water as a stock solution and then diluted in ACSF to a final concentration before use. KN93 (2-[*N*-(2-hydroxyethyl)-*N*-(4-methoxybenzenesulfonyl)]amino-*N*-(4-chlorocinnamyl)-*N*-methylbenzylamine) was obtained from Merck (Darmstadt, Germany) and directly dissolved in ACSF.

Electrode implantation and in vivo *priming.* In some experiments, priming stimulation was applied *in vivo* to electrodes implanted into the lateral perforant path (see below, electrode implantation), with a subsequent analysis of synaptic plasticity *in vitro*. Seven to 8-week-old male Wistar rats underwent electrode implantation into the dentate gyrus as described previously (Kulla et al., 1999). Briefly, under sodium pentobarbitone anesthesia (Nembutal, 40 mg/kg, i.p., Serva Feinbiochemica, Heidelberg, Germany), animals underwent implantation of a monopolar recording electrode into the dentate gyrus granule cell layer and of a bipolar stimulating electrode into the lateral perforant path. Electrodes were made from 0.1-mm-diameter Teflon-coated stainless steel wire. A drill hole was made (1.0 mm diameter) for the recording electrode (3.1 mm posterior to bregma, 1.9 mm lateral to the midline), and a second drill hole (1 mm diameter, 7.9 mm posterior to bregma, and 5 mm lateral to the midline) was made for the stimulating electrode. The dura was pierced through both holes, and the recording and stimulating electrodes were lowered into the dentate gyrus granule cell layer and the lateral perforant path, respectively. Recordings of evoked field potentials via the implanted electrodes were taken throughout surgery. As a criterion for the lateral perforant path origin of the fEPSPs, we verified that double-pulse stimulation (interpulse interval of 40 ms) caused paired-pulse facilitation. Only animals in which clear paired-pulse facilitation was observed were used for the present experiments. Once verification of the location of the electrodes was complete, the entire assembly was sealed and fixed to the skull with dental acrylic (Paladur; Heraeus Kulzer, Mainz, Germany). The animals were allowed between 7 and 10 d to recover from surgery before experiments commenced.

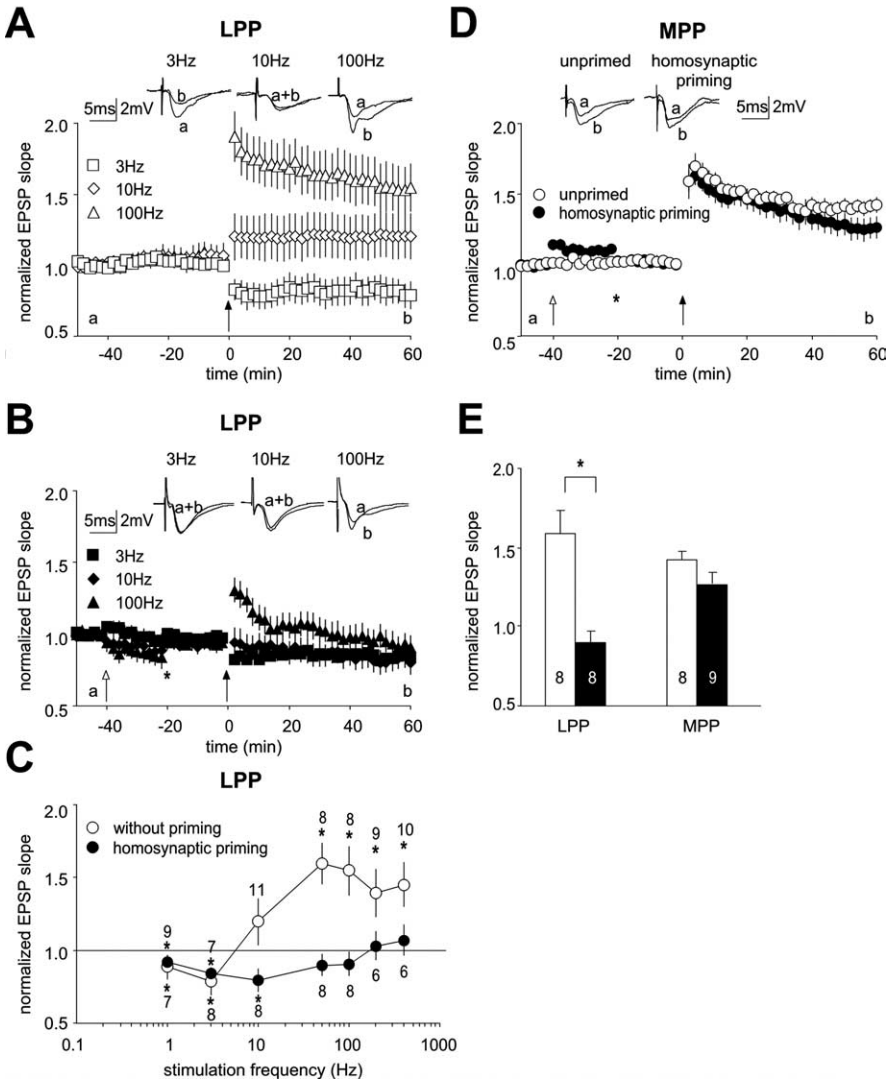

Figure 1. Homosynaptic priming inhibits subsequent LTP at the lateral perforant path (LPP) but not the medial perforant path (MPP). ***A***, ***B***, Time course of the fEPSP slope measured at the lateral perforant pathway, with (***B***) or without (***A***) 10 Hz priming applied to the same pathway (open arrow in ***B***). Averaged experiments with conditioning tetani of 3 Hz (squares), 10 Hz (diamonds), and 100 Hz (triangles) are depicted (filled arrows in ***A*** and ***B***). Asterisks in ***B*** and ***D*** indicate time points at which stimulation strength was adjusted to yield EPSPs of baseline amplitude. Insets, Sample traces obtained at the time points indicated by the lowercase letters. ***C***, Summary of the amount of synaptic plasticity measured 60 min after application of the conditioning tetanus. The frequencies of conditioning stimulations were varied from 1 to 400 Hz. Numbers near the data points indicate the number of experiments. Asterisks indicate significant differences in fEPSP slope when compared with the baseline fEPSP slope. ***D***, Time course of the fEPSP slope measured at the medial perforant pathway, with (filled circles) or without (open circles) 10 Hz priming applied to the medial perforant path (time point indicated by the open arrow). A 50 Hz tetanus was applied as conditioning stimulus (filled arrow). Insets represent sample traces obtained at the time points indicated by the lowercase letters. ***E***, Summary of the amount of synaptic plasticity measured 60 min after application of the conditioning tetanus after homosynaptic priming in the lateral and medial perforant paths with 50 Hz conditioning pulses. Numbers within the bars indicate the number of slices. Asterisk indicates significant difference for the lateral perforant path but not the medial perforant path.

For application of priming stimuli, electrodes were connected to an amplifier and stimulus isolator via a flexible cable in all animals, and the baseline stimulation strength was adjusted as described for the *in vitro* experiments. In one group of animals, priming stimulation with a protocol identical to the one described above (see above, Priming and conditioning stimuli) at a simulation strength increased twofold compared with baseline was applied (primed group). A control group of animals was handled identically, but no priming stimulus was applied. In all *in vivo* experiments, we verified immediately before application of priming that clear paired-pulse facilitation was observed in the stimulated pathway. On average, the ratio of the second to the first EPSP amplitude was 1.29 ± 0.01. Experiments were consistently conducted at the same time of day (commencing at 8:00 A.M.). Animals were maintained on a 12 h light/dark cycle. When slices were prepared from these animals, care was taken to visualize electrode position during preparation. Ipsilaterally to the side of electrode placement, the slices immediately adjacent to the one containing the electrode track were chosen for recording. Cutting slices comprising both hemispheres allowed us to select exactly corresponding slices on the contralateral side. In an additional group of animals, the effects of priming *in vivo* on lateral and medial perforant path EPSPs measured subsequently *in vivo* for up to 24 h was tested to exclude that priming stimulation *in vivo* induced long-lasting changes in synaptic strength.

Results

Frequency dependence of synaptic plasticity at the lateral perforant path

It is well established that the amount of synaptic potentiation or depression varies as a nonmonotonic function with the strength of synaptic activation at many synapses. We have therefore initially examined the amount of synaptic plasticity elicited with conditioning stimulation of varying frequencies at the lateral perforant path (10 trains of 20 pulses spaced 1 s apart, frequencies of pulses within trains ranging from 1 to 400 Hz). Similar to previous studies, we found that low frequencies of 1 and 3 Hz induced LTD [3 Hz (square symbols in Fig. 1*A*), 0.79 ± 0.09 normalized fEPSP slope; $n = 8$], whereas higher frequencies resulted in expression of LTP [100 Hz (Fig. 1*A*, triangles), normalized fEPSP slope 1.55 ± 0.17; $n = 8$]. Conditioning stimulation with 10 Hz caused only low levels of potentiation (normalized fEPSP slope, 1.19 ± 0.16; $n = 11$), indicating that the crossover point between LTD and LTP is close to this stimulation frequency. The results obtained with the whole range of different conditioning frequencies are shown in Figure 1*C* (open symbols, numbers of experiments shown for each data point, significant differences to baseline EPSP slope indicated by asterisks).

Homosynaptic priming inhibits subsequent LTP at the lateral perforant path

We next addressed the question whether priming stimulation alters synaptic plasticity at the lateral perforant path. To this end, we used a stimulation protocol identical to those used in Figure 1*A*, at a frequency of 10 Hz. We chose this protocol because it did not cause significant long-term changes in synaptic transmission. After establishing a stable baseline, a 10 Hz priming stimulation was applied (Fig. 1*B*, open arrow). Forty minutes after priming, we tested the potential of the lateral perforant path to exhibit synaptic plasticity using the same range of conditioning stimula-

tions as in Figure 1*A*. Clearly, priming stimulation caused a dramatic loss in the ability of lateral perforant path synapses to undergo potentiation. As shown in Figure 1*B*, conditioning stimulations at 100 Hz did not induce long-term potentiation (normalized fEPSP slope 1 h after tetanization, 0.91 ± 0.08; $n = 8$). The stimulation frequencies of 3 and 10 Hz caused depression (normalized fEPSP slope, 0.84 ± 0.03, $n = 7$ and 0.8 ± 0.08, $n = 8$, respectively). So far, these results indicate a dramatic loss of LTP, with LTD at low stimulation frequencies remaining intact (summarized in Fig. 1*C*, significant differences to baseline fEPSP slope indicated by asterisks). Significant differences between primed and control groups were found at conditioning frequencies of 50 and 100 Hz. We also tested whether inhibition of LTP by previous priming lasts for longer than 40 min, as depicted in Figure 1*A–C*. To this end, we prolonged the interval between homosynaptic 10 Hz priming and conditioning stimulation to the lateral perforant path to 2 h. After this longer postpriming interval, we still observed a significant priming-induced reduction in LTP (unprimed slices, normalized fEPSP slope 1 h after tetanization, 1.33 ± 0.04, $n = 7$; primed slices, normalized fEPSP slope, 1.13 ± 0.03, $n = 8$; $p < 0.05$).

Homosynaptic priming does not affect subsequent LTP at the medial perforant path

The medial perforant path shows a termination area onto dentate granule cell dendrites that is distinct from the lateral perforant path. Specifically, medial perforant path synapses are formed on the proximal dentate granule cell dendrites within the middle molecular layer, whereas the lateral perforant path terminates within the outer portion of the molecular layer. This segregation is thought to have functional implications for information processing and plasticity in the dentate gyrus. Consistent with this possibility, significant differences in short- and long-term synaptic plasticity have been observed in these two pathways (McNaughton, 1980; Dahl and Sarvey, 1990). We therefore examined whether homosynaptic priming also affects the potential to express LTP in the medial perforant path. To this end, we used a conditioning frequency at which pronounced priming effects were observed in the lateral perforant path [50 Hz (Fig. 1*C*)]. As shown in Figure 1*D*, 10 Hz priming performed 40 min before conditioning stimulation caused only small effects on the amount of LTP (unprimed, 1.42 ± 0.05 normalized fEPSP slope, $n = 8$; 10 Hz primed, 1.27 ± 0.08 normalized fEPSP slope, $n = 9$). No statistical difference was found between the two groups. Although we did not examine conditioning stimulations over the whole range of frequencies tested for the lateral perforant path, these results suggest that the potential to exhibit priming-induced metaplasticity of LTP is much lower at medial perforant path synapses (see comparison of lateral and medial perforant path for conditioning stimulations of 50 Hz in Fig. 1*E*).

Heterosynaptic priming of the medial perforant path inhibits subsequent LTP at the lateral perforant path

Having established that the lateral perforant path displays significant homosynaptic priming effects, we further examined the conditions under which such effects can be elicited. The dentate gyrus afforded us with the opportunity to test whether priming can be induced heterosynaptically because the two anatomically distinct aspects of the perforant path can be functionally discriminated *in vitro*. As described previously (Dietrich et al., 1997), we positioned a pair of stimulating and recording electrodes within the outer and middle molecular layer of the dentate gyrus for lateral and medial perforant path recordings, respectively. Electrode positions were adjusted to yield clear current sinks in the outer and sources within the middle molecular layer for lateral perforant path stimulation and vice versa for medial perforant path stimulation (Fig. 2*A*, left). Furthermore, fEPSPs in the lateral perforant path showed paired-pulse facilitation, whereas those in the medial perforant path displayed paired-pulse inhibition (interpulse interval of 40 ms). As an additional criterion, we applied the group III metabotropic glutamate receptor agonist L-AP-4 (10 μM) at the end of each experiment. L-AP-4 selectively inhibited only lateral but not medial perforant path responses [fEPSP reduction by 26.4 ± 4.8%, $n = 13$ in the lateral perforant path and −0.5 ± 2.5%, $n = 13$ in the medial perforant path (Fig. 2*A*, right)]. Any recordings that did not fulfill these criteria were excluded from additional analysis.

Once baseline recording was established in this configuration, a 10 Hz priming stimulation was applied to the medial perforant path (Fig. 2*B*, open arrows), which did not affect lateral perforant path responses (Fig. 2B_1). Forty minutes after priming to the medial perforant path, a 50 Hz conditioning stimulation was applied to the lateral perforant path (Fig. 2B_1, filled arrow). The amount of LTP induced in the lateral perforant path by this conditioning stimulation was significantly reduced after heterosynaptic priming (normalized fEPSP slope, 1.01 ± 0.04; $n = 6$; $p < 0.05$) compared with unprimed control slices in the same recording configuration [normalized fEPSP slope, 1.39 ± 0.06; $n = 7$ (Fig. 2B_1,*C*)]. These data are in good agreement with published data, in which priming applied to the medial perforant path *in vivo* raised the threshold for induction of lateral perforant path LTP (Abraham et al., 2001). These findings indicate that heterosynaptic metaplasticity at these pathways is a robust phenomenon present both *in vivo* and *in vitro*. It should be noted that, unlike the study published by Abraham et al. (2001), the priming protocols used in the present study did not affect basal synaptic transmission (Fig. 2B_2). Likewise, application of the conditioning 50 Hz stimulation to the lateral perforant path failed to cause large changes in the medial perforant path fEPSPs (Fig. 2B_2).

Priming stimulation either *in vitro* or *in vivo* induces a long-lasting inhibition of LTP at the lateral perforant path

An examination of time intervals >8 h between priming and conditioning stimulation is difficult *in vitro* because of possible changes in recording conditions. We therefore opted for another approach to determine whether priming effects persist for >12 h. We stereotactically implanted stimulation electrodes unilaterally into the lateral perforant path of intact rats. After appropriate recovery periods (see Materials and Methods), 10 Hz priming stimulation identical to that used in the *in vitro* experiments was delivered *in vivo* to the lateral perforant path (*in vivo* priming) (Fig. 3*A*,*C*). A control group of animals was connected to the stimulus isolator and handled identically to primed animals but without application of the priming stimulation (sham priming) (Fig. 3*A*,*C*). Sixteen to 18 h after *in vivo* priming or sham priming, animals were killed, and hippocampal slices were prepared with a vibratome as described for the above experiments. After equilibration in the interface chamber for ~1 h and baseline recording, conditioning stimulation was applied to the lateral perforant path using the same protocol as for the *in vitro* experiments (50 Hz, average time from application of priming/sham priming to *in vitro* induction of LTP, 17.8 ± 0.9 h, $n = 10$ and 16.3 ± 0.6 h, $n = 12$, respectively; NS).

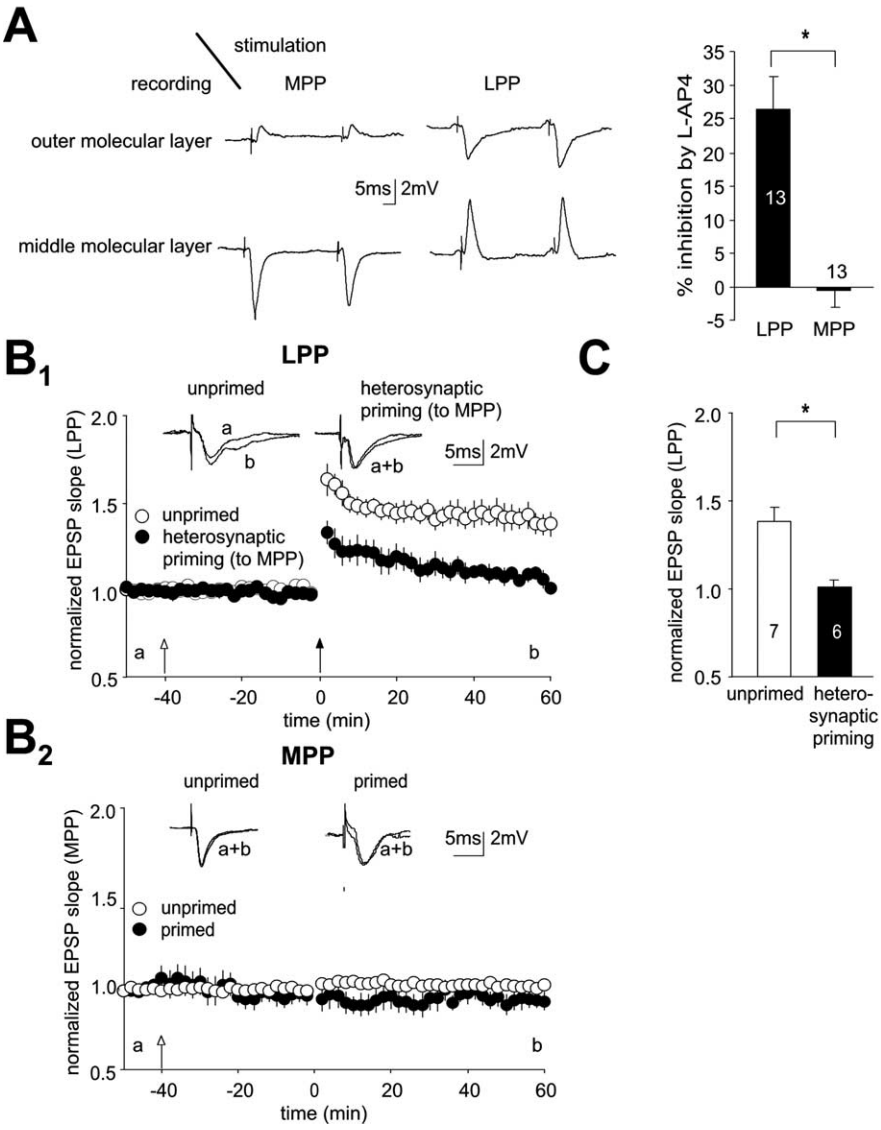

Figure 2. Heterosynaptic priming applied to the medial perforant path (MPP) inhibits subsequent LTP at the lateral perforant path (LPP). ***A***, Recording configuration (left panel) for simultaneous recording of lateral and medial perforant path fEPSPs. Medial perforant path stimulation within the middle molecular layer resulted in a current sink in the middle molecular layer and a current source in the outer molecular layer (leftmost traces). Lateral perforant path stimulation within the outer molecular layer resulted in a current sink in the outer molecular layer and a source in the middle molecular layer (rightmost traces). Paired-pulse stimulation (40 ms interpulse interval) revealed paired-pulse inhibition within the medial perforant path and paired-pulse facilitation within the lateral perforant path. Pharmacological verification (right panel) of the identity of lateral versus medial perforant path fEPSPs. fEPSP slope inhibition (percentage) by the mGluR group III agonist L-AP-4 (10 μM, 20 min application at the end of experiments) was compared between the lateral and medial perforant paths. Numbers of slices are shown within or above each bar throughout the figures, and significant difference is indicated by an asterisk. ***B*$_1$** depicts the time course of the fEPSP slope measured at the lateral perforant pathway, with (filled circles) or without (open circles) 10 Hz priming applied to the medial perforant path (time point indicated by the open arrow). A 50 Hz tetanus to the lateral perforant path was used as a conditioning stimulus (filled arrow). ***B*$_2$** illustrates the time course of simultaneously recorded fEPSPs at the medial perforant path. Insets represent sample traces obtained at the time points indicated by the lowercase letters in both panels. ***C***, Summary of the amount of synaptic plasticity measured 60 min after application of the conditioning tetanus. Asterisks indicate significant differences in LTP in unprimed slices (open bars) and slices that underwent heterosynaptic priming protocols (filled bars).

Because the *in vivo* priming stimulation was performed unilaterally, we separately analyzed the hippocampi ipsilateral and contralateral to the stimulation electrode. The hippocampus implanted with the stimulation electrode showed a remarkable decrease of LTP after priming stimulation (normalized fEPSP slope, 1.12 ± 0.04; $n = 4$; $p < 0.05$), whereas robust LTP was evoked in sham-primed animals (1.5 ± 0.05; $n = 6$) (Fig. 3*A*). Interestingly, a significant but less pronounced effect of priming was observed on the contralateral side (primed group, 1.19 ± 0.04 normalized fEPSP slope, $n = 6$; sham-primed animals, 1.39 ± 0.05, $n = 6$; $p < 0.05$) (Fig. 3*B*). These experiments are summarized in Figure 3*C*. Because unilateral application priming stimulation *in vivo* caused reduction of LTP in both hippocampi, these findings also imply the existence of heterosynaptic priming effects, possibly via commissural fibers. These results presented in Figure 3 suggest that the priming-induced profound loss of LTP is strikingly stable, lasting at least 2 h *in vitro* and up to 16–18 h *in vivo*. Metaplasticity lasting for several hours *in vitro* has been seen previously (Holland and Wagner, 1998). Moreover, *in vivo* analyses have shown that some forms of metaplasticity induced in the dentate gyrus may persist for several days after priming stimulation (Abraham et al., 2001).

To exclude that 10 Hz priming stimulation itself caused LTP *in vivo* that might occlude later LTP *in vitro*, we monitored the long-term effects of 10 Hz priming stimulation *in vivo*. Application of the 10 Hz priming stimulation *in vivo* did not cause significant long-term changes in lateral perforant path synaptic efficacy compared with sham-primed animals either after 1 h (primed, 0.97 ± 0.02, $n = 7$; sham primed, 1.03 ± 0.02, $n = 9$) or after 24 h (primed, 1.12 ± 0.06, $n = 7$; sham primed, 1.00 ± 0.03, $n = 9$; NS). The medial perforant path behaved differently. Medial perforant path priming caused a significant transient reduction in synaptic efficacy at medial perforant pathway immediately after conclusion of the priming stimulation (primed, 0.50 ± 0.065, $n = 4$; sham primed, 0.97 ± 0.02, $n = 10$; $p < 0.001$), which returned to baseline values 2 h after priming and remained unaltered thereafter (24 h after priming, primed, 1.08 ± 0.05, $n = 4$; sham primed, 0.99 ± 0.03, $n = 10$; NS)

NMDA receptors and postsynaptic cell firing in the induction of metaplasticity

It has been proposed that Ca^{2+} influx into postsynaptic neurons is the key trigger for the induction of metaplasticity. Entry of Ca^{2+} may arise via either synaptic Ca^{2+}-permeable receptors, most probably NMDA receptors, or voltage-gated Ca^{2+}-permeable channels during action potential firing. We first examined whether NMDA receptors are required for the induction of this form of metaplasticity. We blocked NMDA receptors with D-APV during priming stimulation [25 μM for 30 min before priming (application indicated by horizon-

tal bar in Fig. 4*A*)] and subsequently applied a 10 Hz priming stimulation. After 40 min of perfusion with normal ACSF, a 50 Hz conditioning stimulation was applied to elicit LTP. As shown in Figure 4*A*, LTP was successfully induced in both primed (normalized fEPSP slope, 1.45 ± 0.08; $n = 8$) and unprimed (normalized fEPSP slope, 1.49 ± 0.07; $n = 7$) groups, with no significant difference between the two groups (Fig. 4*B*). Thus, as seen previously for other forms of priming stimulation (Huang et al., 1992), induction of metaplasticity with 10 Hz stimulation relies on the activation of NMDA receptors.

Although NMDA receptors appear necessary for synaptic induction of metaplasticity, it could be that an important effect of NMDA receptor activation is facilitation of synaptically driven postsynaptic firing (Abraham et al., 2001). In this case, eliciting postsynaptic action potentials might also be an effective stimulus for induction of metaplasticity. We therefore induced granule cells to fire action potentials by antidromic stimulation with a 10 Hz priming paradigm identical to that used for synaptic priming. To exclude that the antidromic stimulation might recruit progressively less granule neurons during the course of 10 Hz stimulation, we measured the amplitude of the antidromic population spike during priming stimulation. The amplitudes of the antidromic population spikes elicited by the first and 20th stimulus during priming, however, did not reveal a reduction in amplitude (20th population spike 97.42% of first population spike; $n = 9$; data not shown). Application of antidromic priming stimulation caused some depression of lateral perforant path EPSPs, similar to although less pronounced than LTD induced by antidromic stimulation in other preparations (Christofi et al., 1993). Antidromic priming also resulted in a potent inhibition of subsequent LTP (1.16 ± 0.03; $n = 9$; $p < 0.05$) compared with unprimed control recordings (normalized fEPSP slope, 1.59 ± 0.14; $n = 8$), similar to homosynaptic and heterosynaptic priming (Fig. 1*E*, 2*C*). It should be noted that, although most of the granule cell activity will arise from the antidromically evoked action potentials, we cannot completely exclude some degree of synaptic activation during the antidromic priming stimulation by activation of hilar axons. Nevertheless, this experiment suggests that the average rate of postsynaptic cell firing can be a criti-

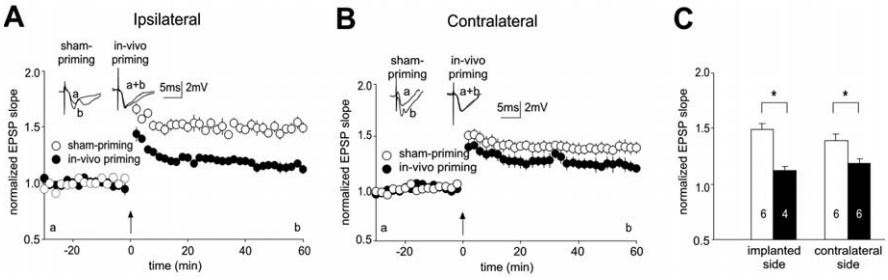

Figure 3. Priming stimulation induces a long-lasting inhibition of LTP at the lateral perforant path. ***A***, ***B***, Time course of *in vitro* experiments with conditioning stimuli of 50 Hz to the lateral perforant path (filled arrows). In one set of experiments, priming stimulation had been applied previously *in vivo* (16–18 h before *in vitro* LTP induction) to the lateral perforant path (filled circles). As a control group, animals were handled identically, but no priming stimulation was delivered (sham priming; open circles). *In vivo* priming was performed unilaterally 16–18 h before performing *in vitro* recording. ***A*** depicts recordings from the ipsilateral hippocampus, and ***B*** summarizes recordings from the contralateral hippocampus. Insets represent sample traces obtained at the time points indicated by the lowercase letters. ***C***, Summary of the amount of synaptic plasticity measured 60 min after application of the conditioning tetanus. Open and filled bars represent sham-priming and primed groups, respectively. Numbers of slices are shown within each bar, and asterisks indicate significant differences.

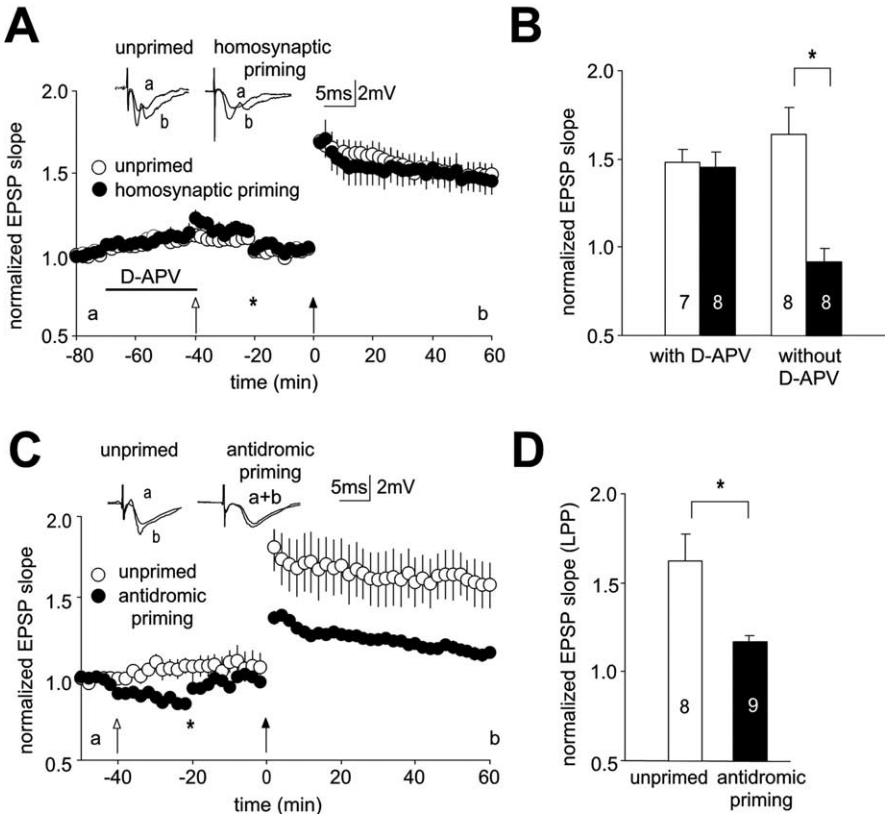

Figure 4. Induction of metaplasticity via NMDA receptors versus postsynaptic cell firing. ***A***, Time course of the fEPSP slope measured at the lateral perforant pathway, with (filled circles) or without (open circles) 10 Hz priming applied to the same pathway (open arrow). The NMDA receptor antagonist D-APV (25 μM) was applied during the time indicated by the horizontal line. A 50 Hz conditioning tetanus (filled arrow) to the lateral perforant path was applied for induction of LTP. Asterisks (***A***, ***C***) indicate time points at which stimulation strength was adjusted to yield EPSPs of baseline amplitude. Insets represent sample traces obtained at the time points indicated by the lowercase letters. Note that similar LTP was obtained in primed and unprimed slices. ***B***, Comparison of the amount of LTP 60 min after the conditioning tetanus when priming was applied in the presence of D-APV (leftmost bars) or under control conditions (rightmost bars; corresponding to data from Fig. 1*C* shown for comparison). Open and filled bars represent sham-priming and primed groups, respectively. Numbers of slices are shown within each bar. Asterisk indicates significant difference. ***C***, Time course of the fEPSP slope measured at the lateral perforant pathway, with (filled circles) or without (open circles) 10 Hz antidromic priming (time point indicated by the open arrow). A 50 Hz tetanus to the lateral perforant path was used as a conditioning stimulus (filled arrow). Insets represent sample traces obtained at the time points indicated by the lowercase letters. ***D***, Summary of the amount of LTP measured 60 min after application of the conditioning tetanus. Asterisks indicate significant differences in LTP in unprimed slices (open bars) and slices that underwent antidromic priming protocols (filled bars).

cal integration mechanism for adjusting subsequent synaptic plasticity, as proposed previously (Bienenstock et al., 1982; Abraham et al., 2001).

Autophosphorylation of αCaMKII at Thr305/306 is required for metaplasticity at the lateral perforant path

It has been shown recently that autophosphorylation of αCaMKII at Thr305/306 is important for regulating the CaMKII association with the postsynaptic density and for setting the threshold for LTP induction in naive slices (Elgersma et al., 2002). Therefore, this could be an attractive mechanism to control metaplasticity at the lateral perforant path. To test the involvement of CaMKII Thr305/306 phosphorylation in metaplasticity at the lateral perforant path, we used mice in which the Thr305 and Thr306 amino acids of endogenous αCaMKII are substituted by nonphoshorylatable residues (valine and alanine, respectively, TT305/6VA mutation) (Elgersma et al., 2002) (see Materials and Methods). In these mice, αCaMKII cannot undergo inhibitory autophosphorylation. We predicted that the priming-induced inhibition of LTP at the lateral perforant path should be significantly reduced in these animals if priming requires inhibitory Thr305/306 autophosphorylation. Because LTP levels with tetani at 50 Hz were not fully saturated in mice (data not shown), as opposed to rats (Fig. 1), we used 100 Hz conditioning stimuli for these experiments. In wild-type mice, application of this tetanus led to stable LTP after 1 h (1.35 ± 0.06; $n = 9$) (Fig. 5*A*, open symbols, *C*). The effects of previous application of a priming stimulus was very similar to that observed in rats: LTP was considerably diminished to 1.10 ± 0.04 ($n = 9$; $p < 0.05$) (Fig. 5*A*, filled symbols, *C*). In marked contrast, Thr305/306VA mice exhibited completely unaltered LTP levels after priming (unprimed, 1.33 ± 0.04, $n = 7$ vs primed, 1.33 ± 0.04, $n = 7$, respectively) (Fig. 5*B*,*C*). It is of note that the levels of LTP in wild-type and Thr305/306VA mice were comparable, indicating that the capacity for expression of LTP per se is intact in mutant mice. It is also unlikely that the thresholds for the induction of LTP are altered in mutant mice. We addressed this question by analyzing synaptic transmission after 10 Hz stimulation (see Materials and Methods). This stimulation paradigm corresponds to the threshold at which LTD transitions to LTP (θ_m). A 10 Hz stimulation did not cause significant changes in basal synaptic transmission in either wild-type (0.98 ± 0.07 compared with pre-10 Hz baseline, 40 min after stimulation; $n = 12$) or mutant (1.04 ± 0.09; $n = 12$) mice. Collectively, these results provide strong evidence that 10 Hz priming dramatically reduces the potential for LTP induction in the lateral perforant path via inhibitory autophosphorylation of αCaMKII at Thr305/306.

CaMKII activity is required for LTP in the lateral but not the medial perforant path

These experiments raise the question why metaplasticity is observed in the lateral but not the medial perforant path. One possibility that might account for this pathway-specific phenomenon is that CaMKII activity is required for LTP only in the lateral but not the medial perforant path. In this case, a reduction of CaMKII activity by inhibitory autophosphorylation during priming would not be expected to reduce subsequent LTP in the medial perforant path. We tested this idea by examining the effects of inhibiting CaMKII with KN93 (10 μM) on LTP in the medial versus lateral perforant path. Indeed, inhibition of CaMKII caused a marked reduction of LTP in the lateral perforant path (1.35 ± 0.06, $n = 9$ under control conditions vs 1.06 ± 0.04, $n = 8$ in the presence of KN93; $p < 0.05$) (Fig. 6*A*,*B*).

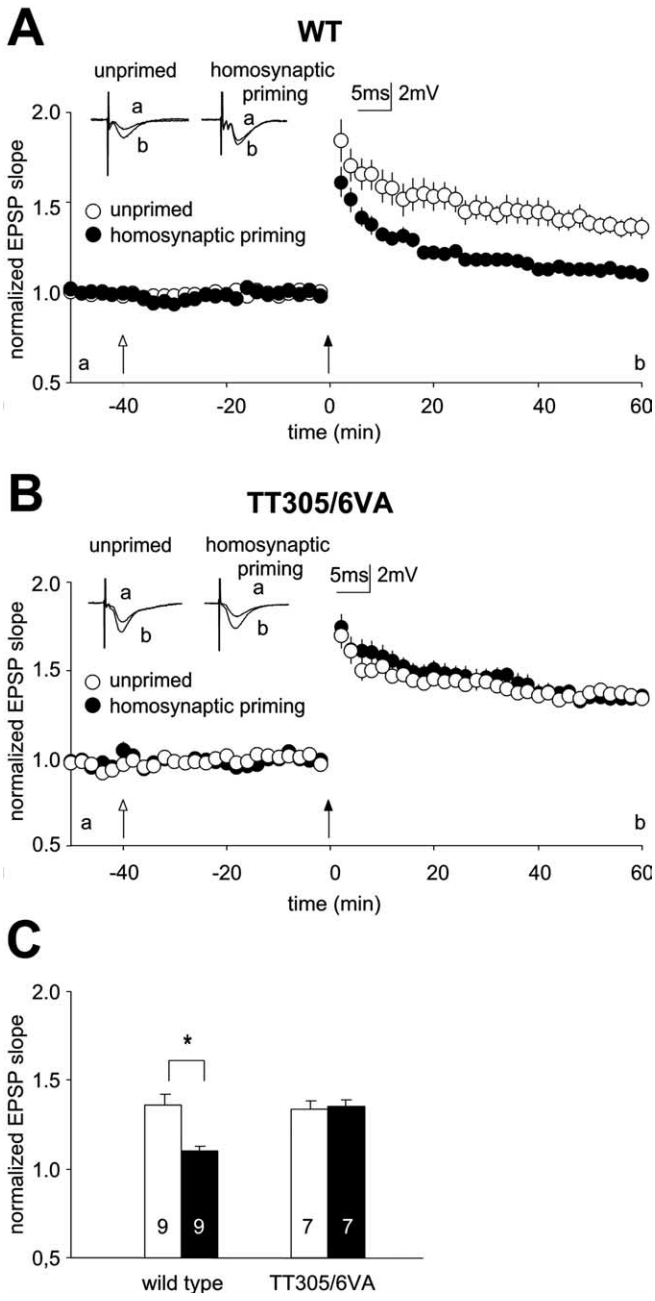

Figure 5. Inhibitory autophosphorylation of αCaMKII at Thr305/306 is required for metaplasticity. ***A***, Experiments in wild-type mice (WT). Time course of the fEPSP slope measured at the lateral perforant pathway, with (open symbols) or without (filled symbols) 10 Hz priming applied to the same pathway (time point of priming indicated by open arrows in ***A*** and ***B***). Conditioning tetani of 100 Hz were used (filled arrows in ***A*** and ***B***). Insets, Sample traces obtained at the time points indicated by the lowercase letters. ***B***, Priming experiment in mice expressing a modified αCaMKII in which Thr305 and 306 were substituted by nonphoshorylatable amino acids (TT305/6VA mice). Symbols as in ***A***. Note the absence of a difference between the primed and unprimed groups (filled and open symbols, respectively). ***C***, Summary of the amount of synaptic plasticity measured 60 min after application of the conditioning tetanus. Asterisk indicates significant difference.

In marked contrast, inhibiting CaMKII did not significantly affect LTP elicited in the medial perforant path (1.37 ± 0.07 under control conditions vs 1.22 ± 0.05 in the presence of KN93; $n = 5$ in both groups) (Fig. 6*C*,*D*).

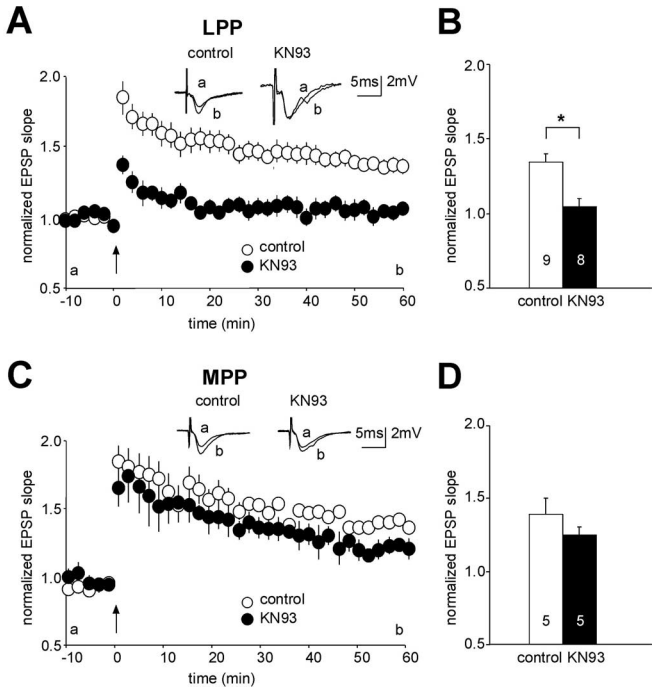

Figure 6. CaMKII is required for LTP in the lateral perforant path (LPP) but not the medial perforant path (MPP). ***A***, Time course of the fEPSP slope measured at the lateral perforant pathway of C57BL/6 mice, with (filled symbols) or without (open symbols) application of KN93 (10 μM). A conditioning tetanus of 100 Hz was used (filled arrow). Insets, Sample traces obtained at the time points indicated by the lowercase letters. ***B***, Summary of the amount of synaptic plasticity measured 60 min after application of the conditioning tetanus at the lateral perforant pathway. Open and filled bars represent control and KN93-treated groups, respectively. Numbers of slices are shown within each bar, and asterisk indicates significant differences. ***C***, Time course of the fEPSP slope measured at the medial perforant pathway, with (filled symbols) or without (open symbols) application of KN93 (10 μM). A conditioning tetanus of 100 Hz was used (filled arrow). Insets, Sample traces obtained at the time points indicated by the lowercase letters. ***D***, Summary of the amount of synaptic plasticity measured 60 min after application of the conditioning tetanus at the medial perforant pathway. Open and filled bars represent control and KN93-treated groups, respectively. Numbers of slices are shown within each bar, and asterisk indicates significant differences.

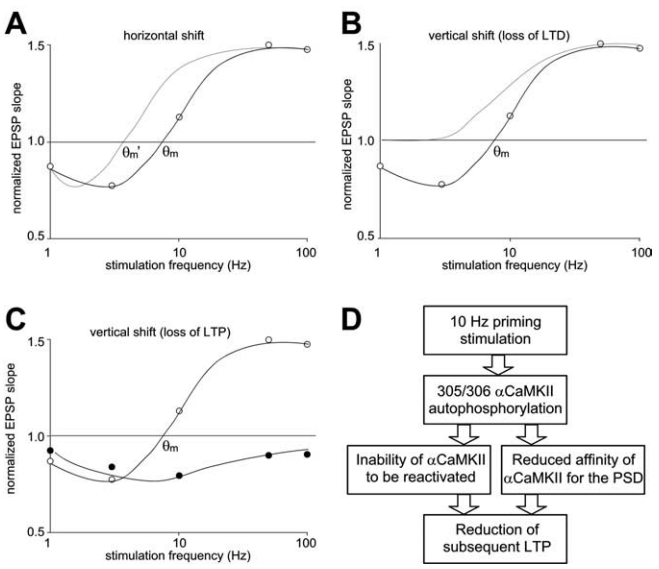

Figure 7. Implications for the sliding threshold model of synaptic plasticity. ***A***, Classical model in which the correlate of metaplasticity is a change in the threshold between LTD and LTP (θ_m). Such an effect may occur without a change in the maximal levels of LTD or LTP. Rather, it is expressed as a shift in θ_m after induction of metaplasticity (shown as θ_m') and a corresponding horizontal shift in the BCM curve (Bienenstock et al., 1982). ***B***, ***C***, Loss of LTD (***B***) with maintained levels of LTP appears to occur in visual cortex (Philpot et al., 2003). In the present study, priming resulted in loss of LTP but maintained levels of LTD (***C***). Both forms of metaplasticity in ***B*** and ***C*** are expressed as a vertical shift in the BCM curve and a decreased range of synaptic strength that can be exhibited by the synapse. Data points shown are from the present study (see Fig. 1*C*, open circles, without priming and filled circles, after 10 Hz priming). The lines shown in ***A–C*** are for illustrative purposes only. ***D***, Proposed mechanism underlying priming-induced suppression of LTP. A 10 Hz priming induces CaMKII autophosphorylation at Thr305/306 in the calcium/calmodulin domain, which in turn prevents subsequent reactivation of the enzyme to full activity as well as causing a strong reduction in CaMKII affinity to the PSD. These mechanisms may, in concert, underlie the observed reduction of subsequent LTP.

Discussion

Many CNS synapses appear to encode previous activity not only as changes in synaptic strength but also as a change in the potential to subsequently exhibit LTP or LTD. This phenomenon has been termed metaplasticity. In our experiments, we describe metaplasticity in the lateral perforant path invoked by stimulation at 10 Hz (close to θ_m), expressed as a dramatic and long-lasting loss in subsequent LTP in the lateral perforant path. A similar decrease in the potential to express LTP after priming stimulations that do not change basal synaptic transmission has been observed previously in the CA1 region (Huang et al., 1992; Larkman et al., 1992; O'Dell and Kandel, 1994). Alternatively, priming stimulation with high-frequency trains was performed in the presence of NMDA receptor antagonists to prevent the induction of LTP, with similar results (Wang and Wagner, 1999). Evidence of metaplasticity induced without changes in basal synaptic transmission in other hippocampal synapses has so far been limited (Christie and Abraham, 1992). Remarkably, in the present study, priming affected only subsequent lateral perforant path LTP but not LTD. Changes in LTD elicited with associative but not nonassociative stimulation protocols have been shown previously to occur only within a narrow frequency range, being present with priming frequencies of 5 Hz but not 1 or 15 Hz (Christie and Abraham, 1992). This raises the intriguing possibility that specific forms of metaplasticity may be invoked depending on the priming frequency band.

In the classical view, the expression mechanism of metaplasticity underlying these phenomena was thought to be a shift in θ_m, with the maximal amount of depression and potentiation left unchanged (Bienenstock et al., 1982; Bear et al., 1987) (Fig. 7*A*). Our results, as well as changes observed after visual deprivation in rats (Kirkwood et al., 1996), suggest that metaplasticity may also be expressed as a change in the maximal amount of LTD or LTP synapses can exhibit. In the visual cortex, visual deprivation causes marked loss of LTD, whereas LTP is left intact (Kirkwood et al., 1996) (depicted schematically in Fig. 7*B*). In our experiments, priming caused loss of LTP, with LTD left intact (depicted in Fig. 7*C*). In contrast to the purely "horizontal shift" in θ_m, these forms of metaplasticity may be described as a "vertical shift" in the Bienenstock–Cooper–Munro (BCM) curve (Philpot et al., 2003), leading to loss of either LTP or LTD.

Mechanisms underlying metaplasticity in the lateral perforant path

As reported previously in the CA1 region (Huang et al., 1992), as well as in the dentate gyrus (Abraham et al., 2001), metaplasticity induced by synaptic 10 Hz priming proved to be dependent on the activation of NMDA receptors. Thus, NMDA receptor-mediated Ca^{2+} influx appears to contribute to intracellular Ca^{2+} transients required for both induction of metaplasticity and LTP.

However, this does not appear to be an absolute requirement, because antidromic priming in the absence of synaptic stimulation also induced metaplasticity in our experiments. Indeed, metaplasticity can be evoked even in the presence of NMDA receptor blockers if the intensity of the priming stimulation is sufficiently high (Wang and Wagner, 1999). The most parsimonious explanation for these results is that the absence of NMDA-mediated synaptic transmission can be compensated by other Ca^{2+} influx pathways. Moreover, the induction of metaplasticity with antidromic priming suggests that postsynaptic action potentials are sufficient to induce metaplasticity even in the complete absence of synaptic stimulation (Abraham et al., 2001).

Several studies have implied that CaMKII may be an attractive candidate to control metaplasticity (Abraham and Tate, 1997; Tompa and Friedrich, 1998; Elgersma et al., 2004). Indeed, CaMKII appears to be well suited to allow bidirectional shifts in synaptic plasticity thresholds. This capability of CaMKII likely hinges on the complex phosphorylation-dependent regulation of CaMKII at two major regulatory sites, Thr286 and Thr305/306. The current view holds that strong synaptic activation, such as during a high-frequency tetanus, causes binding of Ca^{2+}/calmodulin to CaMKII subunits and subsequent translocation from the actin cytoskeleton to the postsynaptic density. Sufficient levels of Ca^{2+}/calmodulin cause autophosphorylation at Thr286, which dramatically increases the affinity for Ca^{2+}/calmodulin and enables the holoenzyme to remain autonomously active even after Ca^{2+} levels have decayed (for review, see Lisman et al., 2002). As long as Ca^{2+}/calmodulin is bound to CaMKII, phosphorylation at the Thr305/306 sites is inhibited because these sites are located within the Ca^{2+}/calmodulin binding domain of CaMKII. After translocation to the postsynaptic density, CaMKII then binds to the NR2B subunit of the NMDA receptor (Bayer et al., 2001). This binding has several major consequences. First, it causes autonomous CaMKII activity that is not dependent on the phosphorylation state of the kinase, as well as trapping of calmodulin. Moreover, binding to the NR2B subunit blocks subsequent phosphorylation at Thr305/306. Thus, a large increase of postsynaptic Ca^{2+}/calmodulin (e.g., during high-frequency tetanization) cannot immediately result in the subsequent inhibition of CaMKII activity by Thr305/306 autophosphorylation. Indeed, our experiments using mutant mice expressing αCaMKII that cannot undergo inhibitory autophosphorylation show that blockade of inhibitory autophosphorylation does not influence the maximal levels of LTP at lateral perforant path synapses obtained with strong tetanic stimulation.

Conversely, our experiments do demonstrate a pivotal role of inhibitory Thr305/306 autophosphorylation for expression of priming-induced metaplasticity. How could subthreshold priming stimuli efficiently induce Thr305/306 autophosphorylation? A likely explanation is that subthreshold priming stimulation leads to activation of only few CaMKII subunits within the entire holoenzyme. This would be insufficient to activate CaMKII to a level that it can move to the PSD and bind to the NR2B subunit of the NMDA receptor. In fact, CaMKII may even fail to dissociate from the actin cytoskeleton because this process requires Ca^{2+}/calmodulin binding (Shen et al., 1998; Shen and Meyer, 1999). In this scenario, subsequent dissociation of Ca^{2+}/calmodulin from CaMKII subunits would permit phosphorylation of these subunits at Thr305/306. This phosphorylation has two important consequences. First, although this CaMKII may have some autonomous activity attributable to a small amount of Thr286 phosphorylation, Thr305/306 phosphorylation abolishes the ability to be fully reactivated, because T305/306 phosphorylation interferes with Ca^{2+}/calmodulin binding (Hashimoto et al., 1987; Colbran and Soderling, 1990; Patton et al., 1990; Mukherji and Soderling, 1994). More importantly, *in vitro* as well as *in vivo* studies have demonstrated that Thr305/306 phosphorylation of αCaMKII strongly reduces the affinity of αCaMKII to the postsynaptic density (Strack et al., 1997; Shen et al., 2000; Elgersma et al., 2002). The association of αCaMKII with the postsynaptic density, in turn, is thought to be essential for the expression of LTP (Hu et al., 1999; Lisman and Zhabotinsky, 2001; Elgersma et al., 2002). Because phosphorylation at Thr305/306 has a strong dominant-negative effect (Elgersma et al., 2002), Thr305/306 phosphorylation of only a few subunits may be sufficient to prevent PSD association of the CaMKII holoenzyme. Thus, although a subsequent stimulus of 100 Hz may induce Thr286 phosphorylation at the remaining subunits that are not blocked by previous Thr305/306 phosphorylation, this is apparently not sufficient to overcome the PSD dissociating properties of the subunits within the holoenzyme that are phosphorylated at Thr305/306. This mechanism would readily explain why subthreshold activation causes phosphorylation at Thr305/306 and why this, in turn, powerfully inhibits subsequent LTP.

Our results are also in good agreement with experiments performed in other types of αCaMKII mutant mice. Mice expressing αCaMKII that mimics inhibitory phosphorylation display a dramatic reduction in LTP and learning (Elgersma et al., 2002). Similarly, because phosphorylation at Thr305/306 occurs rather efficiently (Elgersma et al., 2002), the observed shift toward LTD in the Thr286Asp mice expressing autonomously activated CaMKII (Mayford et al., 1995) could also be attributable to increased Thr305/306 phosphorylation in these mice. We did not observe changes in LTD after priming stimulation, suggesting that this CaMKII-dependent mechanism does not affect the mechanisms underlying long-term depression of synaptic responses. Indeed, either genetic or pharmacological inhibition of CaMKII (Kirkwood et al., 1997; Lee et al., 2000) or genetic manipulation of inhibitory autophosphorylation fails to alter the levels of LTD (Elgersma et al., 2002). Although our results suggest that priming-induced modulation of αCaMKII association with the PSD may be a key contributor to metaplasticity (Fig. 7*D*), the data do not exclude that additional enzymatic pathways may also play a role in metaplasticity at other synapses, as has been suggested for protein phosphatases (Zeng et al., 2001; Woo and Nguyen, 2002). It is an intriguing possibility that protein phosphatase pathways might affect αCaMKII and, by extension, CaMKII-dependent metaplasticity. In addition, we should note that, although inhibitory autophosphorylation of αCaMKII appears to be required for metaplasticity expressed during the first hour after priming, we cannot exclude that additional, downstream mechanisms may be involved in metaplasticity expressed at longer latencies after priming.

Pathway specificity of priming effects

Intriguingly, priming stimulations that readily induced metaplasticity in the lateral perforant path failed to do so in the medial perforant path, although the lateral and medial perforant paths terminate on the same postsynaptic target. In principle, such a pathway specificity may arise in two ways. First, inhibitory autophosphorylation of CaMKII could be induced only in the lateral

but not the medial perforant path. Such a difference might arise via expression of different types of NMDA receptors or Ca^{2+} channels, giving rise to local differences in priming-induced Ca^{2+} increases. Downstream of Ca^{2+} influx pathways, it might be that inhibitory autophosphorylation occurs at both the medial and lateral perforant paths, but that CaMKII activity is not required for LTP induction at the medial perforant path. Indeed, we found that blocking CaMKII with KN93 completely inhibited LTP at the lateral perforant path while only weakly affecting LTP at the medial perforant path. This idea is in good agreement with recent work showing that medial perforant path LTP is only affected if either p42/44 mitogen-activated protein kinase or protein kinase A are blocked in addition to CaMKII (Wu et al., 2004). These results indicate that loss of CaMKII activity can be compensated by other kinases in the medial but not the lateral perforant pathway. More generally, the requirement for different sets of kinases at individual synaptic pathways may constitute an attractive mechanism to generate pathway-specific and stimulation-paradigm-specific modulation of synaptic plasticity.

References

Abraham WC, Bear MF (1996) Metaplasticity: the plasticity of synaptic plasticity. Trends Neurosci 19:126–130.

Abraham WC, Tate WP (1997) Metaplasticity: a new vista across the field of synaptic plasticity. Prog Neurobiol 52:303–323.

Abraham WC, Mason-Parker SE, Bear MF, Webb S, Tate WP (2001) Heterosynaptic metaplasticity in the hippocampus in vivo: a BCM-like modifiable threshold for LTP. Proc Natl Acad Sci USA 98:10924–10929.

Bayer KU, De Koninck P, Leonard AS, Hell JW, Schulman H (2001) Interaction with the NMDA receptor locks CaMKII in an active conformation. Nature 411:801–805.

Bear MF, Cooper LN, Ebner FF (1987) A physiological basis for a theory of synapse modification. Science 237:42–48.

Bienenstock EL, Cooper LN, Munro PW (1982) Theory for the development of neuron selectivity: orientation specificity and binocular interaction in visual cortex. J Neurosci 2:32–48.

Bortolotto ZA, Bashir ZI, Davies CH, Collingridge GL (1994) A molecular switch activated by metabotropic glutamate receptors regulates induction of long-term potentiation. Nature 368:740–743.

Christie BR, Abraham WC (1992) Priming of associative long-term depression in the dentate gyrus by θ frequency synaptic activity. Neuron 9:79–84.

Christie BR, Stellwagen D, Abraham WC (1995) Reduction of the threshold for long-term potentiation by prior theta-frequency synaptic activity. Hippocampus 5:52–59.

Christofi G, Nowicky AV, Bolsover SR, Bindman LJ (1993) The postsynaptic induction of nonassociative long-term depression of excitatory synaptic transmission in rat hippocampal slices. J Neurophysiol 69:219–229.

Cohen AS, Raymond CR, Abraham WC (1998) Priming of long-term potentiation induced by activation of metabotropic glutamate receptors coupled to phospholipase C. Hippocampus 8:160–170.

Colbran RJ, Soderling TR (1990) Calcium/calmodulin-independent autophosphorylation sites of calcium/calmodulin-dependent protein kinase II. Studies on the effect of phosphorylation of threonine 305/306 and serine 314 on calmodulin binding using synthetic peptides. J Biol Chem 265:11213–11219.

Dahl D, Sarvey JM (1990) β-Adrenergic agonist-induced long-lasting synaptic modifications in hippocampal dentate gyrus require activation of NMDA receptors, but not electrical activation of afferents. Brain Res 526:347–350.

Deisseroth K, Bito H, Schulman H, Tsien RW (1995) Synaptic plasticity: a molecular mechanism for metaplasticity. Curr Biol 5:1334–1338.

Dietrich D, Beck H, Kral T, Clusmann H, Elger CE, Schramm J (1997) Metabotropic glutamate receptors modulate synaptic transmission in the perforant path: pharmacology and localization of two distinct receptors. Brain Res 767:220–227.

Elgersma Y, Fedorov NB, Ikonen S, Choi ES, Elgersma M, Carvalho OM, Giese KP, Silva AJ (2002) Inhibitory autophosphorylation of CaMKII controls PSD association, plasticity, and learning. Neuron 36:493–505.

Elgersma Y, Sweatt JD, Giese KP (2004) Mouse genetic approaches to investigating calcium/calmodulin-dependent protein kinase II function in plasticity and cognition. J Neurosci 24:8410–8415.

Giese KP, Fedorov NB, Filipkowski RK, Silva AJ (1998) Autophosphorylation at Thr286 of the alpha calcium-calmodulin kinase II in LTP and learning. Science 279:870–873.

Hashimoto Y, Schworer CM, Colbran RJ, Soderling TR (1987) Autophosphorylation of Ca^{2+}/calmodulin-dependent protein kinase II. Effects on total and Ca^{2+}-independent activities and kinetic parameters. J Biol Chem 262:8051–8055.

Holland LL, Wagner JJ (1998) Primed facilitation of homosynaptic long-term depression and depotentiation in rat hippocampus. J Neurosci 18:887–894.

Hu B-R, Fux CM, Martone ME, Zivin JA, Ellisman MH (1999) Persistent phosphorylation of cyclic AMP responsive element-binding protein and activating transcription factor-2 transcription factors following transient cerebral ischemia in rat brain. Neuroscience 89:437–452.

Huang Y-Y, Colino A, Selig DK, Malenka RC (1992) The influence of prior synaptic activity on the induction of long-term potentiation. Science 255:730–733.

Kirkwood A, Rioult MC, Bear MF (1996) Experience-dependent modification of synaptic plasticity in visual cortex. Nature 381:526–528.

Kirkwood A, Silva A, Bear MF (1997) Age-dependent decrease of synaptic plasticity in the neocortex of alphaCaMKII mutant mice. Proc Natl Acad Sci USA 94:3380–3383.

Kulla A, Reymann KG, Manahan-Vaughan D (1999) Time-dependent induction of depotentiation in the dentate gyrus of freely moving rats: involvement of group 2 metabotropic glutamate receptors. Eur J Neurosci 11:3864–3872.

Larkman A, Hannay T, Stratford K, Jack J (1992) Presynaptic release probability influences the locus of long term potentiation. Nature 360:70–72.

Lee HK, Barbarosie M, Kameyama K, Bear MF, Huganir RL (2000) Regulation of distinct AMPA receptor phosphorylation sites during bidirectional synaptic plasticity. Nature 405:955–959.

Lisman J, Schulman H, Cline H (2002) The molecular basis of CaMKII function in synaptic and behavioural memory. Nat Rev Neurosci 3:175–190.

Lisman JE, Zhabotinsky AM (2001) A model of synaptic memory: a CaMKII/PP1 switch that potentiates transmission by organizing an AMPA receptor anchoring assembly. Neuron 31:191–201.

Manahan-Vaughan D, Reymann KG (1996) Metabotropic glutamate receptor subtype agonists facilitate long-term potentiation within a distinct time window in the dentate gyrus in vivo. Neuroscience 74:723–731.

Mayford M, Wang J, Kandel ER, O'Dell TJ (1995) CaMKII regulates the frequency-response function of hippocampal synapses for the production of both LTD and LTP. Cell 81:891–904.

McNaughton BL (1980) Evidence for two physiologically distinct perforant pathways to the fascia dentata. Brain Res 199:1–19.

Mukherji S, Soderling TR (1994) Regulation of Ca^{2+}/calmodulin-dependent protein kinase II by inter- and intrasubunit-catalyzed autophosphorylations. J Biol Chem 269:13744–13747.

O'Dell TJ, Kandel ER (1994) Low-frequency stimulation erases LTP through an NMDA receptor-mediated activation of protein phosphatases. Learn Mem 1:129–139.

Patton BL, Miller SG, Kennedy MB (1990) Activation of type II calcium/calmodulin-dependent protein kinase by Ca^{2+}/calmodulin is inhibited by autophosphorylation of threonine within the calmodulin-binding domain. J Biol Chem 265:11204–11212.

Philpot BD, Espinosa JS, Bear MF (2003) Evidence for altered NMDA receptor function as a basis for metaplasticity in visual cortex. J Neurosci 23:5583–5588.

Shen K, Meyer T (1999) Dynamic control of CaMKII translocation and localization in hippocampal neurons by NMDA receptor stimulation. Science 284:162–166.

Shen K, Teruel MN, Subramanian K, Meyer T (1998) CaMKIIbeta functions as an F-actin targeting module that localizes CaMKIIalpha/beta heterooligomers to dendritic spines. Neuron 21:593–606.

Shen K, Teruel MN, Connor JH, Shenolikar S, Meyer T (2000) Molecular memory by reversible translocation of calcium/calmodulin-dependent protein kinase II. Nat Neurosci 3:881–886.

Strack S, Choi S, Lovinger DM, Colbran RJ (1997) Translocation of autophosphorylated calcium/calmodulin-dependent protein kinase II to the postsynaptic density. J Biol Chem 272:13467–13470.

Tompa P, Friedrich P (1998) Synaptic metaplasticity and the local charge effect in postsynaptic densities. Trends Neurosci 21:97–102.

Wang H, Wagner JJ (1999) Priming-induced shift in synaptic plasticity in the rat hippocampus. J Neurophysiol 82:2024–2028.

Woo NH, Nguyen PV (2002) "Silent" metaplasticity of the late phase of long-term potentiation requires protein phosphatases. Learn Mem 9:202–213.

Wu J, Rowan MJ, Anwyl R (2004) CaMKII inhibition only blocks LTP induction if combined with inhibition of MAPK or PKA in juvenile rat dentate gyrus. Soc Neurosci Abstr 30:739.2.

Xu L, Anwyl R, Rowan MJ (1998) Spatial exploration induces a persistent reversal of long-term potentiation in rat hippocampus. Nature 394:891–894.

Zeng H, Chattarji S, Barbarosie M, Rondi-Reig L, Philpot BD, Miyakawa T, Bear MF, Tonegawa S (2001) Forebrain-specific calcineurin knockout selectively impairs bidirectional synaptic plasticity and working/episodic-like memory. Cell 107:617–629.